



## Good and bad get together: Inactivation of SARS-CoV-2 in particulate matter pollution from different fuels



José de la Fuente<sup>a,b,\*</sup>, Octavio Armas<sup>c</sup>, Sandra Barroso-Arévalo<sup>d,e</sup>, Christian Gortázar<sup>a</sup>, Teresa García-Seco<sup>d</sup>, Aránzazu Buendía-Andrés<sup>d</sup>, Florentina Villanueva<sup>f,g</sup>, José A. Soriano<sup>c</sup>, Lorena Mazuecos<sup>a</sup>, Rita Vaz-Rodrigues<sup>a</sup>, Reyes García-Contreras<sup>c</sup>, Antonio García<sup>h</sup>, Javier Monsalve-Serrano<sup>h</sup>, Lucas Domínguez<sup>d,e</sup>, José Manuel Sánchez-Vizcaíno<sup>d,e</sup>

<sup>a</sup> SaBio, Instituto de Investigación en Recursos Cinegéticos IREC-CSIC-UCLM-JCCM, Ronda de Toledo s/n, 13005 Ciudad Real, Spain

<sup>b</sup> Department of Veterinary Pathobiology, Center for Veterinary Health Sciences, Oklahoma State University, Stillwater, OK 74078, USA

<sup>c</sup> Escuela de Ingeniería Industrial y Aeroespacial, Universidad de Castilla - La Mancha, Campus de Excelencia Internacional en Energía y Medioambiente, Real Fábrica de Armas, Edif. Sabatini, Av. Carlos III, s/n, 45071 Toledo, Spain

<sup>d</sup> VISAVET Health Surveillance Centre, Universidad Complutense de Madrid, Puerta de Hierro s/n, 28040 Madrid, Spain

<sup>e</sup> Department of Animal Health, Faculty of Veterinary, Universidad Complutense de Madrid, Av. Puerta de Hierro s/n, 28040 Madrid, Spain

<sup>f</sup> Instituto de Investigación en Combustión y Contaminación Atmosférica, Universidad de Castilla La Mancha, Camino de Moledores s/n, 13071 Ciudad Real, Spain

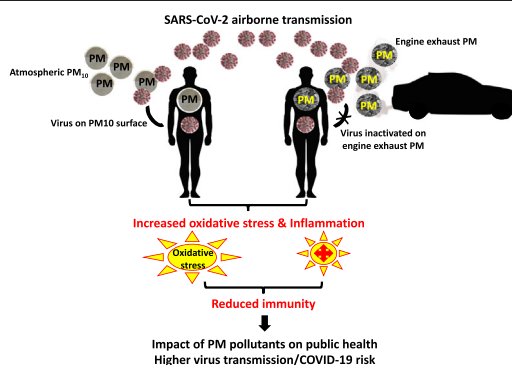
<sup>g</sup> Parque Científico y Tecnológico de Castilla La Mancha, Paseo de La Innovación 1, 02006 Albacete, Spain

<sup>h</sup> CMT-Motores Térmicos, Universitat Politècnica de València, Camino de Vera s/n, 46022 Valencia, Spain

### HIGHLIGHTS

- The question addressed is how long SARS-CoV-2 survives on the surface of different PM.
- We evaluate relationship between fuel and atmospheric PM and virus transmission risk.
- SARS-CoV-2 remains on PM<sub>10</sub> from air pollutants but fuel PM inactivates the virus.
- Pollution PM and particularly fuel PM affect host immunity.
- Atmospheric PM and engine exhaust PM affect oxidative stress and COVID-19.

### GRAPHICAL ABSTRACT



### ARTICLE INFO

Editor: Ewa Korzeniewska

**Keywords:**  
 COVID-19  
 Particulate matter  
 Air pollution  
 Fuel  
 Immunity  
 SARS-CoV-2

### ABSTRACT

Air pollution and associated particulate matter (PM) affect environmental and human health worldwide. The intense vehicle usage and the high population density in urban areas are the main causes of this public health impact. Epidemiological studies have provided evidence on the effect of air pollution on airborne SARS-CoV-2 transmission and COVID-19 disease prevalence and symptomatology. However, the causal relationship between air pollution and COVID-19 is still under investigation. Based on these results, the question addressed in this study was how long SARS-CoV-2 survives on the surface of PM from different origin to evaluate the relationship between fuel and atmospheric pollution and virus transmission risk. The persistence and viability of SARS-CoV-2 virus was characterized in 5 engine exhaust PM and 4 samples of atmospheric PM<sub>10</sub>. The results showed that SARS-CoV-2 remains on the surface of PM<sub>10</sub> from air pollutants but interaction with engine exhaust PM inactivates the virus. Consequently, atmospheric PM<sub>10</sub> levels may increase SARS-CoV-2 transmission risk thus supporting a causal relationship between these factors. Furthermore, the relationship of pollution PM and particularly engine exhaust PM with virus transmission

\* Corresponding author at: SaBio, Instituto de Investigación en Recursos Cinegéticos IREC-CSIC-UCLM-JCCM, Ronda de Toledo s/n, 13005 Ciudad Real, Spain.  
 E-mail address: [josedejesus.fuente@uclm.es](mailto:josedejesus.fuente@uclm.es) (J. de la Fuente).

risk and COVID-19 is also affected by the impact of these pollutants on host oxidative stress and immunity. Therefore, although fuel PM inactivates SARS-CoV-2, the conclusion of the study is that both atmospheric and engine exhaust PM negatively impact human health with implications for COVID-19 and other diseases.

## 1. Introduction

The air pollution in cities is a global problem for society since several pollutant compounds are considered toxic and harmful to the environment and human health (Manisalidis et al., 2020). Air pollution and associated particulate matter (PM) ( $PM_{2.5}$ , aerodynamic diameter  $\leq 2.5 \mu m$ ;  $PM_{10}$ , aerodynamic diameter  $\leq 10 \mu m$ ) has been implicated in the prevalence of pathogens and infectious diseases (Cienciewicki and Jaspers, 2007; Cao et al., 2014; Liu et al., 2018). Due to its relatively smaller size,  $PM_{2.5}$  has greater health impacts because it can penetrate more easily into the respiratory tract, facilitating pathogen access to this tissue (Chen et al., 2016; Comunian et al., 2020). Consequently, inhaled ultrafine PM reach pulmonary alveoli and cause respiratory and systemic diseases (Traboulsi et al., 2017; Feretti et al., 2019). The intense vehicle usage and the high population density in urban areas are the main causes of this environmental impact (von Schneidmesser et al., 2019). In this context, pollutant emissions and mainly PM generated from combustion processes (e.g., vehicles, power and/or heating plants) are considered a factor affecting the appearance of cancer diseases, genetic mutations and/or transmission of infectious diseases (Lewtas, 2007).

Particle matter produced in the combustion process of vehicles, particularly in compression ignition engines, is one of the main contributors to the air pollution of PM. Diesel PM is composed by an insoluble fraction (ISF) formed primarily by soot and other compounds such as salts, water, and inorganic materials (e.g., metals) and by a soluble organic fraction (SOF) mainly composed by hydrocarbons from the fuel and lubricant oil (Prasad and Rao Bella, 2010). Therefore, the main components of the PM are soot and different hydrocarbons that can be condensed and/or adsorbed inside the soot (Prasad and Rao Bella, 2010). Structurally, PM agglomerates are basically formed by primary particles produced during the combustion process by engines (Bockhorn, 1994; Tree and Svensson, 2007; Omidvarborna et al., 2015). Initially, molecules of light hydrocarbons are converted into polycyclic aromatic hydrocarbons (PAHs). Then, soot primary nuclei are formed followed by surface growth (layering) and/or coagulation (increase of particle dimension by joining two or more primary particles). Finally, particles collision with other primary particles forms agglomerates with larger structures that can contain up to 1800 primary particles (Haynes and Wagner, 1981). The composition of PM is also affected by engine characteristics such as category, aging and type of route (e.g., urban, suburban, in traffic) and the (photo)degradation possibly occurring from the emitting source to the targets (e.g., PM half-life) (Argyropoulos et al., 2016; Karjalainen et al., 2016; Gentner et al., 2017; Jaworski et al., 2018). In any case, the definition of PM is in fact determined by its sampling method. Sampling of PM involves drawing a sample of exhaust gas that has been diluted with air and filtering it through sampling filters. However, in this work two types of particulate matter have been used, undiluted soot agglomerates collected inside exhaust duct of the engines and atmospheric collected from the atmosphere.

The coronavirus disease 19 (COVID-19) pandemic caused by severe acute respiratory syndrome coronavirus 2 (SARS-CoV-2) has encouraged research on the effect of air pollution on virus transmission and disease prevalence and symptomatology (Copat et al., 2020; Bourdrel et al., 2021; Maleki et al., 2021). The airborne transmission of SARS-CoV-2 has been demonstrated (Greenhalgh et al., 2021). Epidemiological investigations have related various air pollutants including  $PM_{2.5}$  and  $PM_{10}$  to COVID-19 morbidity and mortality at the population level. This effect may be triggered indirectly through reduction of immune response with increased oxidative stress and its impact on chronic cardiopulmonary diseases and diabetes and directly by PM-virus interactions (Li et al., 2020; Bourdrel et al., 2021; Maleki et al., 2021; Lembo et al., 2021; Atiyani

et al., 2021; Chakraborty et al., 2022; Li et al., 2022). In epidemiological studies conducted in various countries worldwide, an association was found between high  $PM_{2.5}$  values and SARS-CoV-2 viral infections in some regions (Comunian et al., 2020; Pansini and Fornacca, 2021; Maleki et al., 2021). However, these studies have potential biases present in ecological-based analyses of air pollution and COVID-19 causal relationship (Villeneuve and Goldberg, 2022; Bossak and Andritsch, 2022). Other environmental variables such as temperature, relative humidity (RH) and ultraviolet (UV) radiation may also affect SARS-CoV-2 transmission and viability (Lv et al., 2020; Bourdrel et al., 2021; Maleki et al., 2021).

Based on these results, the question addressed in this study was how long SARS-CoV-2 survives on the surface of PM from different origin to evaluate the relationship between engine exhaust and atmospheric pollution and virus transmission risk.

## 2. Materials and methods

### 2.1. Rationale and experimental design of the study

To address the question proposed in this study (Fig. 1A), fuel PM from different origins and atmospheric  $PM_{10}$  were used to evaluate how long SARS-CoV-2 survives on the surface of PM (Fig. 1B and C). In this way, some of the PM were derived from the engine combustion process but collected inside the exhaust duct, while other were collected directly from the atmosphere. Considering that the objective of the study was the characterization of PM-virus interactions, we decided not to use diluted PM to avoid one more factor in the analysis. This is the reason why the study of the effect of PM directly collected from the atmosphere was included to compare the results associated to both types of particles, being the type of fuel the differentiating factor. The persistence and viability of SARS-CoV-2 virus was characterized in 5 fuel PM and in 4 samples of atmospheric  $PM_{10}$  (Table 1). Suspension of SARS-CoV-2 was added to RNase-free and DNase-free ultra-pure water previously incubated with each kind of PM. The 35 mm glass plates were used for containing the virus-PM mixture. Each PM-SARS-CoV-2 interaction was evaluated in triplicate at three different time points, 0 h (T0), 2 h (T1), and 24 h (T2) at 4 °C and 50 % RH (Fig. 1D). Positive (SARS-CoV-2 in RNase/DNase-free water; C+) and negative (RNase/DNase-free water; C-) controls were included. Samples collected at each time point were processed immediately and used for RNA extraction to evaluate SARS-CoV-2 loads by RT-qPCR or cell culture to evaluate virus viability (Fig. 1D).

### 2.2. Engines tested for PM generation

Particulate matter used in this study was produced with two different engines. Engine 1 was a 4 cylinder, 4 stroke, turbocharged, intercooled, 2.2 l Nissan automotive compression ignition engine (Euro 3), equipped with diesel oxidation catalyst (DOC) and common-rail fuel injection system (Soriano et al., 2018). Engine 2 was a commercial medium-duty, 5.1 l, 4 in-line cylinders Volvo engine (Euro VI) compression ignition engine working under Dual-Mode Dual-Fuel (DMDF) mode (Benajes et al., 2017a). The choice of engines used in this study is justified by the following factors: i) although the European car park with diesel engines is decreasing, an important number of vehicles with diesel engines are still working (~25%; <https://www.jato.com>), ii) in a great part of Europe, a non-negligible number of vehicles in use are still Euro 3 (or III), iii) most of the new diesel engines in European vehicles comply with one of the phases of the Euro 6 (or VI) regulation in place before the next Euro 7 (or VII) regulation, and iv) the availability, in terms of the specific type of engine (light, medium or heavy duty), of the participating laboratories is as described above.

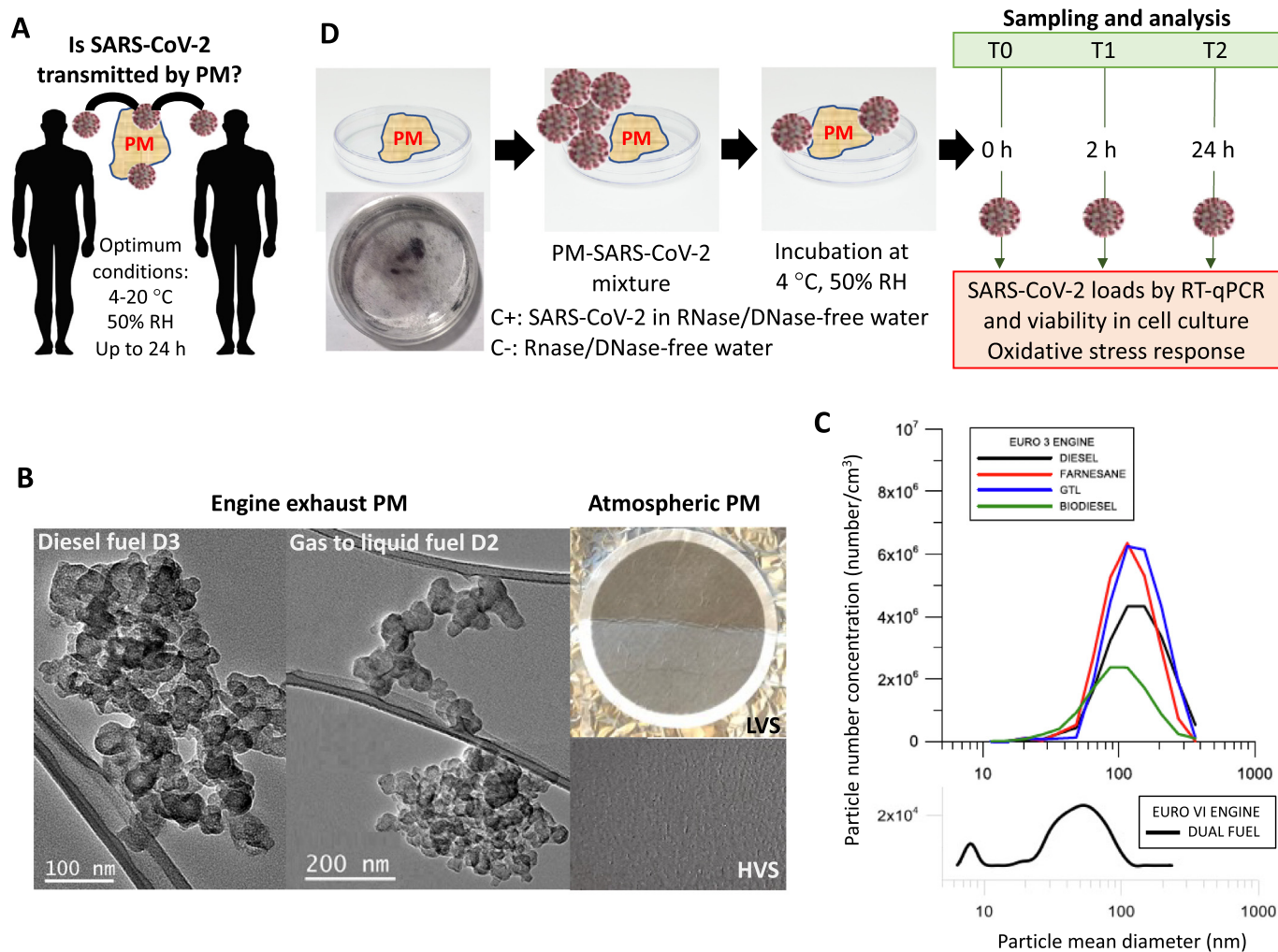


**Fig. 1.** Rationale and experimental design. (A) The question addressed in this study was how long SARS-CoV-2 survives on the surface of PM to evaluate the relationship between fuel and atmospheric pollution and virus transmission risk. (B) Examples of high-resolution transmission electron microscopy (HRTEM) images of soot agglomerates without SOF extraction used in the present work for combustion of diesel and gas to liquid fuels. Images of low-volume sampler (LVS) and high-volume sampler (HVS) filters used to capture atmospheric PM<sub>10</sub> are shown. (C) Particle size distributions at the exhaust pipe of the engines tested. (D) Characterization of the persistence and viability of SARS-CoV-2 in fuel PM and atmospheric PM<sub>10</sub> samples.

### 2.3. Fuels used for PM generation

The fuels used in this study included four for engine 1 (D2-D5; Table 1) and one for engine 2 (D1; Table 1). Samples of PM produced with engine 1 during a typical diesel combustion process of four different fuels were used, (i) ultra-low sulfur diesel fuel, without biodiesel, supplied by Repsol S.A. (Madrid, Spain), (ii) biodiesel fuel blend composed by 72 % soybean and 28 % palm biodiesel (in volume), also supplied by Repsol S.A., (iii) natural gas low temperature Fischer-Tropsch liquid fuel (Gas-to-Liquid GTL fuel), supplied by Sasol Limited (Sandton, South Africa), and (iv) Farnesane fuel, produced through the fermentation of sugar cane biomass by means of genetically modified yeast (*Saccharomyces cerevisiae*) and supplied by the company Amyris Inc. (Emeryville, CA, USA) (Soriano et al., 2018) (Table 1). Sample of PM produced with engine 2 during a DMDF diesel-gasoline low temperature combustion process, were also used. In this case, fuels were an ultra-low sulfur diesel (ULSD) and 95 octane gasoline (Benajes et al., 2017a) (Table 1).

### 2.4. Engine exhaust PM collection and characterization

In both engines, PM samples were collected without air dilution through different stainless-steel homemade particle filters located inside a

recordable cylinder. The PM collection was carried out under steady state modes characteristic of the operation of each engine and their combustion processes. Particle size distribution in PM collected from engine 1 were determined by means of a Nano Scanning Mobility Particle Sizer (Nanoscan SMPS) model 3910 (Soriano et al., 2017) while from engine 2 a SMPS model 3936L75 was used (Benajes et al., 2017b) (Table 1, Fig. 1B–C). In addition, PM collected from engine 1 were also characterized by thermogravimetric analysis (TGA), X-ray diffraction (XRD), Fourier transform infrared spectroscopy (FTIR), Raman spectroscopy (RS) and HRTEM techniques (Soriano et al., 2017) (Table 1). The characteristics of engine exhaust PM were determined for different fuels using data in Fig. 1C, and density equations published before (Gómez et al., 2012; Momenimovahed and Olfert, 2015; Momenimovahed et al., 2021) (Table 1).

### 2.5. Atmospheric PM collection

Atmospheric PM<sub>10</sub> was collected by means of a high-volume sampler (HVS TE-6070DV, Tisch Environmental, Inc., Cleves, OH, USA) and a low-volume sampler (LVS 3.1 Comde-Derenda GmbH, Stahnsdorf, Germany) operating at a flow of 68 m<sup>3</sup> h<sup>-1</sup> and 2.3 m<sup>3</sup> h<sup>-1</sup>, respectively (Fig. 1B). One PM<sub>10</sub> sample was collected onto a quartz fiber filter (QFF, 20.3 × 25.4 cm, Whatman, Maidstone, UK) in the HVS and three PM<sub>10</sub> samples were collected onto glass fiber filters (GFF, 47 mm diameter, Lab

**Table 1**  
Description of the particulate matter used in this study.

PM	Experiment ID	Main characteristics
<i>Engine exhaust PM</i>		
Dual-fuel diesel-gasoline	D1	GMD = 41 nm <sup>a</sup> EC = 0.16 mg/m <sup>3b</sup>
Gas to liquid fuel	D2	GMD = 131 nm <sup>a</sup> EC = 33 mg/m <sup>3c</sup>
Ultra-low sulfur diesel fuel	D3	GMD = 134 nm <sup>a</sup> EC = 35 mg/m <sup>3c</sup>
Farnesane fuel	D4	GMD = 115 nm <sup>a</sup> EC = 23 mg/m <sup>3c</sup>
Palm and soybean biodiesel fuel	D5	GMD = 95 nm <sup>a</sup> EC = 8.9 mg/m <sup>3c</sup>
<i>Soot and atmospheric PM<sub>10</sub></i>		
Filter 1	F1	Collected on 01.12.2021 QFF; mass = 22.21 mg AC = 13.61 µg/m <sup>3</sup>
Filter 2	F2	Collected on 18.11.2021 GFF; mass = 575 µg AC = 10.8 µg/m <sup>3</sup>
Filter 3	F3	Collected on 29.11.2021 GFF; mass = 407 µg AC = 7.6 µg/m <sup>3</sup>
Filter 4	F4	Collected on 30.11.2021 GFF; mass = 1510 µg AC = 28 µg/m <sup>3</sup>

Abbreviations: PM, particulate matter; GMD, geometrical mean diameter; QFF, quartz fiber filter; GFF, glass fiber filter; EC, exhaust particle mass concentration; AC, air particle mass concentration.

<sup>a</sup> Determined from particle size distributions as presented in Fig. 1C.

<sup>b</sup> Determined from particle size distributions using the density equations published in Momenimovahed and Olfert (2015) and Momenimovahed et al. (2021).

<sup>c</sup> Determined from particle size distributions using the density equation published in Gómez et al. (2012).

Logistics Group GmbH, Meckenheim, Germany) in the LVS over 24 h on working days in the small urban area of Ciudad Real located at the heart of Castilla La Mancha region in central-southern Spain. The sampling site was located at the University of Castilla La Mancha (UCLM) area near the main road of the city that surrounds it. Prior to exposure, all filters were conditioned in an oven for 24 h at 250 °C to eliminate any remaining organic matter that was present. Filters were then left in the weighing room (temperature 20 ± 2 °C and RH 42 ± 9 %) for 48 h, before being weighed in triplicate and exposed to the sampling site. After exposure, the filters were returned to the weighing room for 48 h until weighing. Table 1 shows the main characteristics of soot samples and the PM<sub>10</sub> mass and concentration found in the filters.

## 2.6. SARS-CoV-2 virus and Vero E6 cells

SARS-CoV-2 MAD6 isolated from a 69-year-old male patient in Madrid, Spain was kindly provided by Dr. Luis Enjuanes from the National Biotechnology Centre (CNB) at the Higher Council for Scientific Research (CSIC), Spain. Vero E6 cells (ATCC, CRL-158; Manassas, VA, USA) provided by the Carlos III Healthcare Institute, Madrid, Spain, were used to reproduce the SARS-CoV-2 stocks. Cells were incubated at 37 °C under 5 % CO<sub>2</sub> in Gibco Roswell Park Memorial Institute (RPMI) 1640 medium with L-glutamine (Lonza Group Ltd., Basel, Switzerland) and supplemented with 100 IU/ml penicillin, 100 µg/ml streptomycin, and 10 % fetal bovine serum (FBS) (Merck KGaA, Darmstadt, Germany). SARS-CoV-2 titers were determined via a tissue culture infectious dose (TCID<sub>50</sub>) assay.

## 2.7. Experimental approach for the analysis of PM-SARS-CoV-2 interactions

The persistence and viability of SARS-CoV-2 virus was characterized in 5 fuel PM and 4 samples of atmospheric PM<sub>10</sub> (Table 1, Fig. 1D). For this purpose, a suspension of 1 ml of SARS-CoV-2 at 10<sup>5</sup> TCID<sub>50</sub> was added to 1 ml of RNase-free and DNase-free ultra-pure water (ThermoFisher,

Waltham, MA, USA) previously incubated overnight with 4 mg of each type of PM. Although EC and AC were different between both exhaust and air samples (Table 1), the same amount of PM was used for incubation with SARS-CoV-2 to reduce the possible effect of the sample quantity on the results. The 35 mm glass plates were used for containing the virus-PM mixture. Each PM- SARS-CoV-2 interaction was evaluated in triplicate at three different time points, 0 h (T0), 2 h (T1), and 24 h (T2). Plates were incubated at 4 °C and 50 % RH. Controls included positive virus control (C+; 1 ml SARS-CoV-2 at 10<sup>5</sup> TCID<sub>50</sub> plus 1 ml of RNase-free and DNase-free ultra-pure water) and negative control (C-; 2 ml RNase-free and DNase-free ultra-pure water). Samples collected at each time point were processed immediately. The content of each plate was homogenized, collected by pipetting, and deposited in sterile micro centrifuge tubes. Tubes were centrifuged at 3000 RPM for 5 min to allow the separation of the particles and filters. Then, the supernatant was collected and used for subsequent RNA extraction or cell culture.

## 2.8. RNA extraction and reverse transcription-quantitative PCR (RT-qPCR)

SARS-CoV-2-specific RNA was detected using an RT-qPCR assay. Two hundred µl of the collected supernatant were extracted under biosafety level 3 conditions at the VISAVET center in the University Complutense of Madrid, Spain, using the KingFisher Flex System automated extraction instrument (ThermoFisher) using the MagMAX CORE Nucleic Acid Purification Kit (ThermoFisher) according to the manufacturer's instructions. The detection of SARS-CoV-2 RNA was performed targeting the envelope protein (E)-encoding gene (Sarbeco) and two targets (IP2 and IP4) of the RNA-dependent RNA polymerase gene (RdRp) in an RT-qPCR protocol established by the World Health Organization according to the guidelines (<https://www.who.int/emergencies/diseases/novel-coronavirus-2019/technical-guidance/laboratory-guidance>; Corman et al., 2020). The RT-qPCR was carried out using the SuperScript III Platinum One-Step RT-qPCR Kit (ThermoFisher) in a CFX Connect Real-Time PCR Detection System (Bio-Rad, Hercules, CA, USA). A positive cycle threshold (Ct) cut-off of 40 cycles was used with 3 replicates per sample. A result was considered positive when the sample attained a positive result for at least two of the three gene targets analyzed. For subsequent analysis, the average among the three gene targets was used as a unique value of Ct. The RT-qPCR Ct values were compared between PM-SARS-CoV-2 groups for each time point by One-way ANOVA test followed by post-hoc Bonferroni and Holm multiple comparisons (p < 0.05; n = 3 biological replicates; [https://astatsa.com/OneWay\\_Anova\\_with\\_TukeyHSD/](https://astatsa.com/OneWay_Anova_with_TukeyHSD/)).

## 2.9. Evaluation of virus viability in cell culture

The supernatants collected were subjected to virus isolation in African green monkey kidney Vero E6 cells. Cells were cultured in RPMI growth medium supplemented with 10 % FBS, 100 IU/ml penicillin, and 100 µg/ml streptomycin. The cells were seeded in 96-well culture plates and cultured at 37 °C with 5 % CO<sub>2</sub> for 24 to 48 h. Then, cells were inoculated with 10 µl of the PM-SARS-CoV-2 test sample. Mock-inoculated cells were used as negative control. Cultured cells were maintained at 37 °C with 5 % CO<sub>2</sub>, with a daily observation of virus-induced cytopathic effect (CPE) and cell death. After 5 days, cell cultures were frozen, thawed, and subjected to three passages with inoculation of fresh Vero E6 cell cultures with the lysates as described above. SARS-CoV-2 molecular detection was performed by RT-qPCR on the supernatants from every passage to confirm virus viability in cell culture and virus recovery by means of the decrease in the Ct. A positive result for viable virus was considered when cytopathic effect was observed in every passage and virus replication was demonstrated by a decrease in the Ct value obtained by RT-qPCR of the cell supernatant.

## 2.10. Expression levels of oxidative stress response genes

Total RNA was extracted from Vero E6 cells collected at 0 and 24 h after exposure to PM-SARS-CoV-2 at third passage. The mRNA levels of green

monkey (*Chlorocebus sabaues*) genes coding for stress response or related regulatory factor proteins were characterized by RT-qPCR (Table 2). For RT-qPCR, an incubation at 50 °C for 10 min was followed by an initial denaturation step at 95 °C for 1 min, amplification by 40 cycles of 95 °C for 10 s and 60 °C for 1 min using the iTaq Universal SYBR Green One-Step Kit (Bio-Rad, Hercules, USA) and the CFX96 real time PCR system (Bio-Rad). For a total volume of 20 µl, the PCR mixture contained 10 µl of SYBR Green reaction mix, 0.25 µl of iScript reverse transcriptase, 2 µl of forward and reverse primers (10 µM final concentration), 2 µl of RNA sample and 5.75 µl nuclease-free water. For each PCR reaction, every sample had two technical replicates and two negative controls. The Ct values were normalized using the 2<sup>-ΔΔCt</sup> method and expression calculated as the ratio to glyceraldehyde-3-phosphate dehydrogenase (*GAPDH*; F: 5'-GAACGGAA GCTTGTCAATCAATGG-3' and R: 5'-TGTGGTCATGAGTCCTCCACGAT-3'; Korom et al., 2008). The mRNA levels were calculated as the 24 h to 0 h ratio normalized Ct values and compared between 0 and 24 h by Student's *t*-test with unequal variance (*p* < 0.05; *n* = 2 replicates).

### 3. Results and discussion

The SARS-CoV-2 loads in the PM-virus mixtures were assessed using RT-qPCR. The results showed the presence of virus RNA without significant differences between PM-SARS-CoV-2 groups for both engine exhaust PM (Fig. 2A) and atmospheric PM<sub>10</sub> (Fig. 2B). However, when virus viability was assessed by three passages of the collected supernatant in Vero E6 cells, the results showed differences between engine exhaust PM and atmospheric PM<sub>10</sub> (Table 3). While SARS-CoV-2 interaction with atmospheric PM<sub>10</sub> did not affect virus viability, virus replication was not supported as the only suggestion for Filter 1 (decrease in Ct values from 11.80 to 11.32 between 0 and 24 h; Table 3) could be due to methodological differences in RNA levels. However, SARS-CoV-2 interactions with engine exhaust PM resulted in virus inactivation (Table 3). Atmospheric PM<sub>10</sub> were collected in a city with around 74,000 inhabitants, and where traffic is an important source of air pollution (Villanueva et al., 2021). Lara et al. (2022) recently reported after one-year sampling surveillance in this city, that no significant correlation was observed between PAHs and PM<sub>10</sub>, thus suggesting that PM<sub>10</sub> is also formed from non-fuel combustion sources. The PAHs are produced during the incomplete combustion and pyrolysis of organic substances and from unburnt petroleum products, being anthropogenic sources such as traffic, domestic heating, biomass burning, and industrial processes the main sources of PAHs (Oanh et al., 1999; Zielinska et al., 2004; Abbas et al., 2018).

Previous studies conducted during 2012–2013 and 2017–2018 in the atmospheric PM<sub>10</sub> sampling city provided information on PAHs composition (Villanueva et al., 2015; Lara et al., 2022). These studies showed 20 and 109 pg/m<sup>3</sup> average composition of benzo(a)pyrene during 2012–2013 and 2017–2018, respectively. For 5-ring PAHs, the concentration was between 14 and 122 pg/m<sup>3</sup> in 2012–2013 and between 6 and 224 pg/m<sup>3</sup> in 2017–2018. Although the exact composition of PAHs in the samples

collected for this study is not known, the results of previous studies suggest that its content increased in last years. It has been documented that the possible interactions between an adsorbed molecule and a solid surface range from weak nonpolar van der Waals forces to strong chemical bonding. Currently, little is known about the physicochemical mechanisms of the interactions of some viruses such as SARS-Cov-2 with abiotic surfaces and how nonspecific virus-surface interactions affect virus viability and infectiousness (Gerba, 1984; Xin et al., 2021). The absence of correlation between PAHs and PM<sub>10</sub> in the sampling city (Lara et al., 2022), suggested that the composition of the PM<sub>10</sub> is other than mainly soot, probably most related with inorganic composition associated to a low polluted city in a semi-arid region also highly influenced by Saharan intrusions (Díaz et al., 2017). Soot and PM<sub>10</sub> present different composition although PM<sub>10</sub> can content some soot. Due to different surface composition, the interaction with SARS-CoV-2 could also be different and while virus interaction with atmospheric PM<sub>10</sub> did not affect virus viability, interactions with engine exhaust PM resulted in virus inactivation. Additional investigations are needed to understand the nature of the interactions between SARS-CoV-2 and PM<sub>10</sub> engine exhaust PM.

Nevertheless, the results obtained here advanced knowledge of the effect of PM on virus viability, thus providing additional support for epidemiological studies showing a correlation between air pollutants including PM<sub>2.5</sub> and PM<sub>10</sub> and COVID-19 morbidity (Li et al., 2020; Bourdrel et al., 2021; Maleki et al., 2021; Lembo et al., 2021; Atiyani et al., 2021; Chakraborty et al., 2022; Li et al., 2022). Results from previous studies showed that SARS-CoV-2 viruses in droplets and aerosols survive well at low RH of approximately 50 % as opposed to high humidity levels, while the virus remains viable for 5 days at 4 °C, and for 1 day only at 22 °C and 30 °C with virus spread between 5 °C and 15 °C (Fernández-Raga et al., 2021; Maleki et al., 2021). Under the experimental conditions used here (4 °C, 50 % RH, up to 24 h) the virus was viable in atmospheric PM<sub>10</sub>, thus corroborating previous results (Fernández-Raga et al., 2021; Maleki et al., 2021).

Surveillance of SARS-CoV-2 in indoor and outdoor size-segregated PM<sub>10-2.5</sub> samples has shown limited detection of virus RNA in PM<sub>2.5</sub> (Del Real et al., 2022). However, although SARS-CoV-2 RNA has been identified on air pollution PM (Setti et al., 2020; Del Real et al., 2022), virus infectivity is still a question (Woodby et al., 2021). As recently discussed (Woodby et al., 2021), virus incubation with urban PM decreased infectivity for enveloped bacteriophage Φ6 but enhanced infection by nonenveloped Φ174, possibly due to PM damage of lipid membranes in enveloped viruses (Groulx et al., 2018). In a recent mechanistic study, Stapleton et al. (2022) demonstrated that urban PM affects SARS-CoV-2 and human common cold alphacoronavirus 229E (CoV-229E) infectivity by decreasing viral viability while impairing viral inactivation by primary human epithelial cells airway surface liquid (ASL). The results showed for the first time that urban PM consistently inactivated both coronaviruses in vitro, thereby decreasing ambient viral titers before inhalation (Stapleton et al., 2022).

Exposure to PM may have not only a direct but also an indirect role in COVID-19. Fuel PM pollutants affect human health by reducing immune

**Table 2**  
Genes and oligonucleotide primers used for RT-qPCR.

Genes	References	Forward (F) and reverse (R) sequence-specific primers
Nitric oxide synthase (iNOS)	XM_037992776.1	F: 5'-TCCCCATCCAGGCAGCTA-3' R: 5'-TCCACTTGCTGTACTCTGAGGG-3'
Nuclear factor kappa-light-chain-enhancer of activated B cells subunit 1 (NF-kB1, P105)	XM_007997162.2	F: 5'-TCCAGGAGCACAGATGAATTGGA-3' R: 5'-CCAAGGGTGACCGTGCTCAG-3'
NF-kB2 P100	XM_007997163.2	F: 5'-CAGGAGCACAGAGATAATCGACG-3' R: 5'-CAAAGGGTGACCGTGCTCAG-3'
Activator protein 1 (AP-1) component c-FOS	XM_007987321.2 (Mizutani et al., 2006)	F: 5'-CAGAGAGGAGAAACATCTTCCC-3' R: 5'-GATACAATTGAAAATATCCAGCACC-3'
Ap-1 component c-JUN	XM_007978554.2	F: 5'-CCCGAAACTTCAGCACGCAG-3' R: 5'-AGCCATAAGCTCCGCTCTCG-3'
Signal transducer and activator of transcription 1 (STAT1)	XM_007965669.2	F: 5'-GGTACAACATGCTGGTGGCG-3' R: 5'-GGCTGGCGTTAGGACCAAGA-3'
Nuclear factor-erythroid factor 2-related factor 2 (Nrf2)	XM_007965441.2 (Bai et al., 2020)	F: 5'-CTCGTGGAAAAAGAAGTGG-3' R: 5'-CCGTCCAGGAGTTCAGAGAG-3'

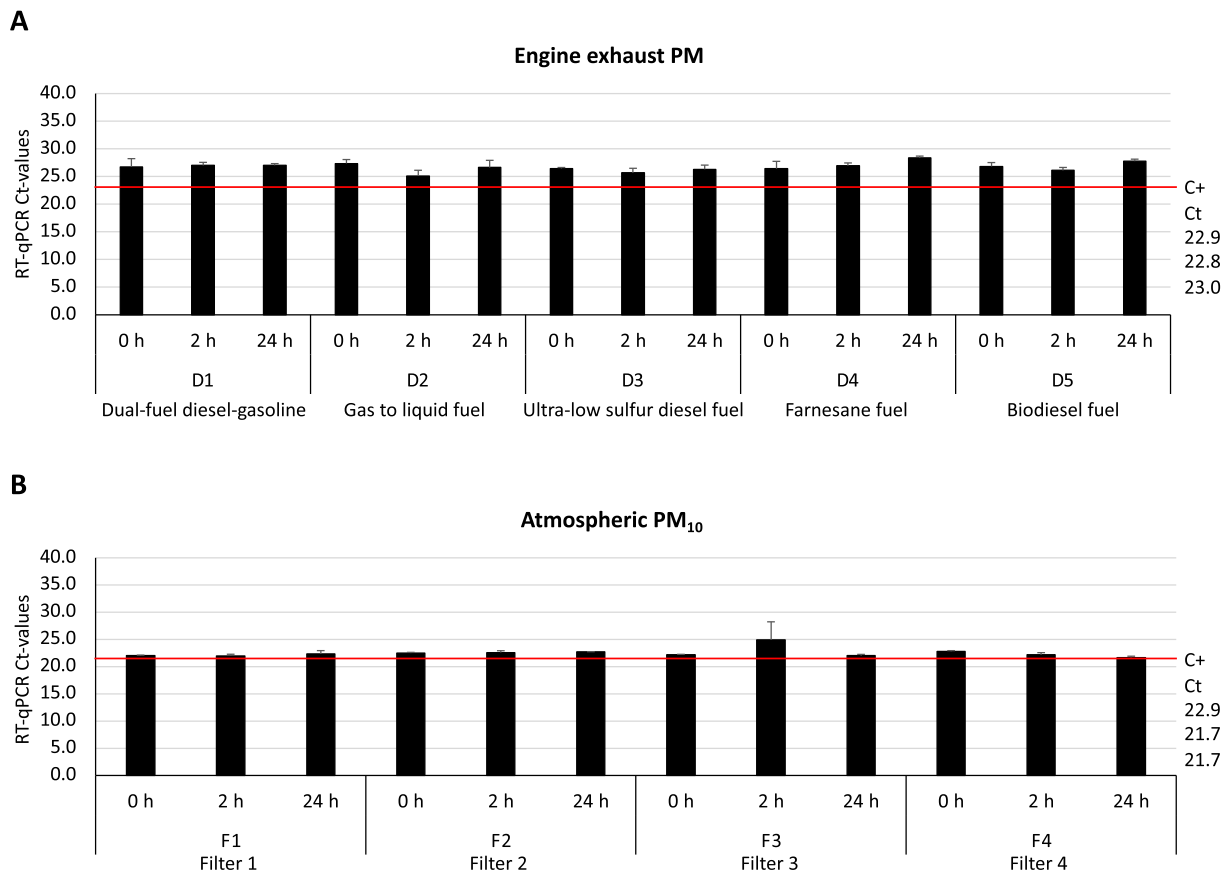


Fig. 2. SARS-CoV-2 loads in PM. The SARS-CoV-2 loads in the PM-virus mixtures after incubation were assessed using RT-qPCR in (A) fuel PM and (B) atmospheric PM<sub>10</sub>. The results (Ave + S.D.) showed presence of virus RNA without differences between PM-SARS-CoV-2 groups (p > 0.05; One-way ANOVA test followed by post-hoc Bonferroni and Holm multiple comparisons). Ct-values for virus positive control (C+) are shown for 0, 2 and 24 h.

response against pathogen infection (Lewtas, 2007; Manisalidis et al., 2020). The PM contain transition metals (Fe, Zn, Ni, and V) that undergo Fenton or Haber-Weiss reactions generating reactive oxygen species (ROS) such as hydrogen peroxide (H<sub>2</sub>O<sub>2</sub>), which reacts with Fe<sup>2+</sup> to produce hydroxyl radical (HO) and promote lipid peroxidation (Woodby et al., 2021). The oxidative stress caused by PM depends on the particle source related to PAHs absorbed on its surface (Woodby et al., 2021). Oxidative stress can limit immune response, cause DNA damage, formation of protein adducts, apoptosis and proinflammatory activation of iNOS and NF-κB, AP-1, STAT1 and Nrf2 transcription factors (Biller-Takahashi et al., 2015; Gangwar et al., 2020; Woodby et al., 2021). Regarding COVID-19, evidence support that PM has a major role in aggravating disease symptoms through different mechanisms affecting host oxidative stress and immune response rather than as carriers of SARS-CoV-2 (e.g., Mescoli et al., 2020; Santurtún et al., 2022).

In this study, the expression of 7 genes coding for stress response or regulatory factors were characterized in Vero E6 cells collected at 0 and 24 h after exposure to PM-SARS-CoV-2 at third passage. Only gene coding for Nrf2 did not produce PCR-positive samples. The results showed that all PM-virus samples except for dual-fuel diesel-gasoline (D1; Table 1) and filter 3 (F3; Table 1) increased cellular oxidative stress and expression levels of oxidative stress response genes (Fig. 3A) (Woodby et al., 2021). The activation of iNOS and/or NF-κB1 with inhibition of NF-κB2 increase ROS production and oxidative stress while inhibiting the expression of antioxidant genes (Fig. 3B). At the same time, the upregulation of genes coding for regulatory factors NF-κB1, AP-1, and/or STAT1 with upregulation/downregulation of NF-κB2 may also increase the risk for inflammatory response negatively affecting immune response (Fig. 3B) (Biller-Takahashi et al., 2015; Gangwar et al., 2020; Woodby et al., 2021; Samanthi, 2021).

Table 3

Results from SARS-CoV-2 viability analysis by cell culture.

PM ID and sampling time point	Virus culture	Ct value in the 3rd passage
Dual-fuel diesel-gasoline D1 0 h	Negative	Negative
Dual-fuel diesel-gasoline D1 2 h	Negative	Negative
Dual-fuel diesel-gasoline D1 24 h	Negative	Negative
Gas to liquid fuel D2 0h	Negative	38.32
Gas to liquid fuel D2 2h	Negative	Negative
Gas to liquid fuel D2 24h	Negative	Negative
Ultra-low sulfur diesel fuel D3 0 h	Negative	Negative
Ultra-low sulfur diesel fuel D3 2 h	Negative	Negative
Ultra-low sulfur diesel fuel D3 24 h	Negative	Negative
Farnesane fuel D4 0 h	Negative	Negative
Farnesane fuel D4 2 h	Negative	Negative
Farnesane fuel D4 24 h	Negative	Negative
Biodiesel fuel D5 0 h	Negative	Negative
Biodiesel fuel D5 2 h	Negative	Negative
Biodiesel fuel D5 24 h	Negative	37.72
Filter 1 F1 0 h	Positive	11.80
Filter 1 F1 2 h	Positive	14.07
Filter 1 F1 24 h	Positive	11.32
Filter 2 F2 0 h	Positive	15.63
Filter 2 F2 2 h	Positive	16.46
Filter 2 F2 24 h	Positive	16.72
Filter 3 F3 0 h	Positive	11.78
Filter 3 F3 2 h	Positive	14.20
Filter 3 F3 24 h	Positive	15.41
Filter 4 F4 0 h	Positive	12.14
Filter 4 F4 2 h	Positive	17.24
Filter 4 F4 24 h	Positive	13.36
Positive virus control C+ 0 h	Positive	14.67
Positive virus control C+ 2 h	Positive	13.85
Positive virus control C+ 24 h	Positive	13.08
Water negative control C- 0 h	Negative	Negative
Water negative control C- 2 h	Negative	Negative
Water negative control C- 24 h	Negative	Negative

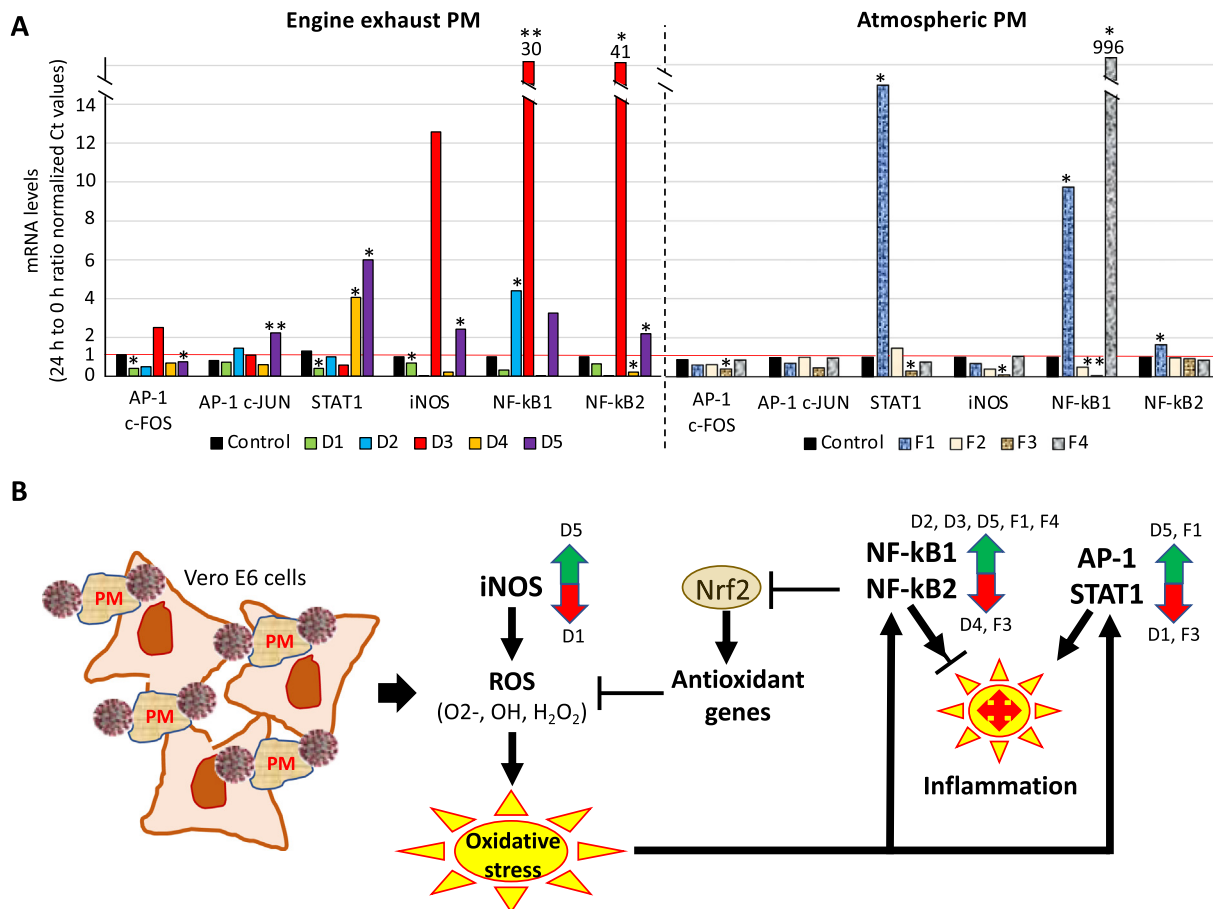


**Fig. 3.** Oxidative stress response to PM-SARS-CoV-2. (A) Expression levels of oxidative stress response genes and regulatory factors. The mRNA levels of oxidative stress response genes iNOS, NF-kB1, NF-kB2, AP-1, and STAT1 were evaluated in Vero E6 cells collected at 0 and 24 h after exposure to PM-SARS-CoV-2 at third passage. The mRNA levels were calculated as the 24 h to 0 h ratio normalized Ct values and compared between 0 and 24 h by Student's *t*-test with unequal variance (\**p* < 0.05, \*\**p* < 0.005; *n* = 2 replicates). (B) Mechanisms activated by oxidative stress response genes and regulatory factors in response to PM-SARS-CoV-2.

However, the incubation with D1 and F3 PMs resulted in a response with potential non oxidative stress capacity through significant reduction in iNOS, NF-kB, STAT1, and/or AP-1 gene-coding expression (Fig. 3A and B). The PM from dual-fuel diesel-gasoline D1 and filter F3 showed the lowest levels of geometrical mean diameter (GMD, 41 nm) and exhaust particle mass concentration (EC, 0.16 mg/m<sup>3</sup>), and air particle mass concentration (AC, 7.6 µg/m<sup>3</sup>), respectively (Table 1). In a recent study, Soriano et al. (2020) concluded that hydrocarbons extracted from soot produced by diesel fuels such as those used here (D2-D5; Table 1) affect cell viability and are genotoxic and mutagenic at different levels. In the current study, the soot corresponding to D1 was obtained from the combustion of a diesel-gasoline blend, where gasoline fraction is 78 %. Accordingly, the PAHs associated to diesel fuel are drastically reduced, a factor that may correlate with the absence of oxidative stress capacity in this soot when compared to D2-D5. In agreement with these results, gasoline particles were reported to increase oxidative DNA damage without a significant effect on oxidative stress in bronchial epithelial cells (Usemann et al., 2018). The lowest level of oxidative stress found in cells exposed to F3 PMs could be related to the smaller concentration of PM<sub>10</sub> found in this sample and thus the likely lower number of compounds causing redox activity (Table 1).

#### 4. Conclusions

The response to the question addressed in this study based on after incubation PM-virus mixtures is that SARS-CoV-2 remains on the surface of PM<sub>10</sub> from air pollutants although with limited replication

capacity while interaction with engine exhaust PM inactivates the virus. Consequently, considering that population is mostly exposed to atmospheric PM secondary particles, atmospheric PM<sub>10</sub> levels may increase SARS-CoV-2 transmission risk thus supporting a causal relationship between these factors. On the contrary, engine exhaust PM inactivates the virus. However, the relationship of pollution PM and particularly diesel engine exhaust PM with virus transmission risk and COVID-19 is also affected by the impact of these pollutants on host oxidative stress response and immunity. Therefore, although fuel PM inactivates SARS-CoV-2, the conclusion of the study is that both atmospheric and engine exhaust PM negatively impact human health with implications for COVID-19 and other diseases. These results showed that engine exhaust PM from different origin consistently inactivated SARS-CoV-2, thus supporting a trade-off between good and bad sides of the PM pollution from different fuels (Fig. 4). The characterization of pathogen interactions with pollution PM is an important component of the One Health approach for reducing the impact of infectious diseases on human and animal health worldwide.

#### CRedit authorship contribution statement

Conceptualization: JF, OA, CG, LD, MSV. Methodology: SBA, TGS, ABA, FV, JAS, LM, RVR, RGC, AG, JMS. Investigation: All authors. Visualization: JF, OA, SBA. Funding acquisition: OA, LD, MSV. Project administration: OA, LD, MSV. Supervision: JF, OA, CG, LD, MSV. Writing – original draft: JF, OA, CG. Writing – review & editing: All authors.

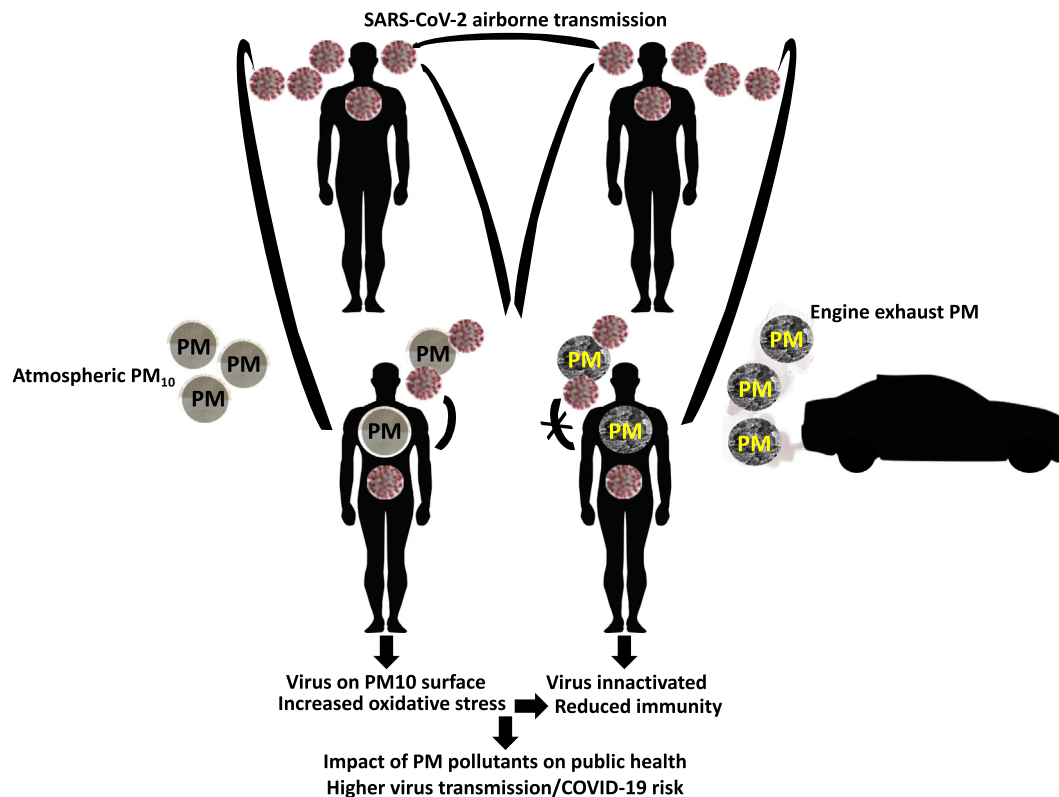


**Fig. 4.** Conclusions of the study. SARS-CoV-2 remains on the surface of PM<sub>10</sub> from air pollutants but interaction with fuel PM inactivates the virus. However, individual exposure to PM and particularly fuel PM may have not only a direct but also an indirect role in COVID-19 by affecting host immune response. Therefore, although fuel PM inactivates SARS-CoV-2, the conclusion of the study is that both atmospheric and fuel PM negatively impact human health with higher risks for virus transmission and COVID-19.

#### Declaration of competing interest

The authors declare that they have no known competing financial interests or personal relationships that could have appeared to influence the work reported in this paper.

#### Acknowledgments

We thank Dr. Luis Enjuanes (CNB-CSIC, Spain) for providing the SARS-CoV-2 isolate. The authors would like to thank the fuel supply by REPSOL, SASOL and AMYRIS companies. Ministry of Science and Innovation project RECOVERY (RTI2018-095923-B-C21) ANTICIPA-UCM REACT-UE-Comunidad de Madrid.

#### References

- Abbas, I., Badran, G., Verdin, A., Ledoux, F., Roumi'e, M., Courcot, D., Garçon, G., 2018. Polycyclic aromatic hydrocarbon derivatives in airborne particulate matter: sources, analysis and toxicity. *Environ. Chem. Lett.* 16, 439–475.
- Argyropoulos, G., Samara, C., Voutsas, D., Kouras, A., Manoli, E., Voliotis, A., Tsakis, A., Chasapidis, L., Konstandopoulos, A., Eleftheriadis, K., 2016. Concentration levels and source apportionment of ultrafine particles in road microenvironments. *Environ. Sci. Technol.* 129, 68–78.
- Atiyani, R., Mustafa, S., Alsari, S., Darwish, A., Janahi, E.M., 2021. Clearing the air about airborne transmission of SARS-CoV-2. *Eur. Rev. Med. Pharmacol. Sci.* 25, 6745–6766.
- Bai, Z., Zhao, X., Li, C., Sheng, C., Li, H., 2020. EV71 virus reduces Nrf2 activation to promote production of reactive oxygen species in infected cells. *Gut Pathog.* 12, 22.
- Benajes, J., García, A., Monsalve-Serrano, J., Boronat, V., 2017a. An investigation on the particulate number and size distributions over the whole engine map from an optimized combustion strategy combining RCCI and dual-fuel diesel-gasoline. *Energy Convers. Manage.* 140, 98–108.
- Benajes, J., García, A., Monsalve-Serrano, J., Boronat, V., 2017b. Gaseous emissions and particle size distribution of dual-mode dual-fuel diesel-gasoline concept from low to full load. *Appl. Therm. Eng.* 120, 138–149.
- Biller-Takahashi, J.D., Takahashi, L.S., Mingatto, F.E., Urbinati, E.C., 2015. The immune system is limited by oxidative stress: dietary selenium promotes optimal antioxidative status

and greatest immune defense in pacu *Piaractus mesopotamicus*. *Fish Shellfish Immunol.* 47, 360–367.

- Bockhorn, H., 1994. *Soot Formation in Combustion*. Springer-Verlag, Berlin.
- Bossak, B.H., Andritsch, S., 2022. COVID-19 and air pollution: a spatial analysis of particulate matter concentration and pandemic-associated mortality in the US. *Int. J. Environ. Res. Public Health* 19, 592.
- Bourdrel, T., Annesi-Maesano, I., Alahmad, B., Maesano, C.N., Bind, M.A., 2021. The impact of outdoor air pollution on COVID-19: a review of evidence from in vitro, animal, and human studies. *Eur. Respir. Rev.* 30, 200242.
- Cao, C., Jiang, W., Wang, B., Fang, J., Lang, J., Tian, G., Jiang, J., Zhu, T.F., 2014. Inhalable microorganisms in Beijing's PM<sub>2.5</sub> and PM<sub>10</sub> pollutants during a severe smog event. *Environ. Sci. Technol.* 48, 1499–1507.
- Chakraborty, S., Dey, T., Jun, Y., Lim, C.Y., Mukherjee, A., Dominici, F., 2022. A spatiotemporal analytical outlook of the exposure to air pollution and COVID-19 mortality in the USA. *J. Agric. Biol. Environ. Stat.* 1–21.
- Chen, R., Hu, B., Liu, Y., Xu, J., Yang, G., Xu, D., Chen, C., 2016. Beyond PM<sub>2.5</sub>: the role of ultrafine particles on adverse health effects of air pollution. *Biochim. Biophys. Acta.* 1860, 2844–2855.
- Ciencewicki, J., Jaspers, I., 2007. Air pollution and respiratory viral infection. *Inhal. Toxicol.* 19, 1135–1146.
- Comunian, S., Dongo, D., Milani, C., Palestini, P., 2020. Air pollution and Covid-19: the role of particulate matter in the spread and increase of Covid-19s morbidity and mortality. *Int. J. Environ. Res. Public Health* 17, 4487.
- Copat, C., Cristaldi, A., Fiore, M., Grasso, A., Zuccarello, P., Signorelli, S.S., Conti, G.O., Ferrante, M., 2020. The role of air pollution (PM and NO<sub>2</sub>) in COVID-19 spread and lethality: a systematic review. *Environ. Res.* 191, 110129.
- Corman, V.M., Landt, O., Kaiser, M., Molenkamp, R., Meijer, A., Chu, D.K., Bleicker, T., Brünink, S., Schneider, J., Schmidt, M.L., Mulders, D.G.J.C., Haagmans, B.L., van der Veer, B., van den Brink, S., Wijsman, L., Goderski, G., Romette, J.L., Ellis, J., Zambon, M., Peiris, M., Goossens, H., Reusken, C., Koopmans, M.P.G., Drosten, C., 2020. Detection of 2019 novel coronavirus (2019-nCoV) by real-time RT-PCR. *Euro Surveill.* 25, 2000045.
- Del Real, A., Expósito, A., Ruiz-Azcona, L., Santibáñez, M., Fernández-Olmo, I., 2022. SARS-CoV-2 surveillance in indoor and outdoor size-segregated aerosol samples. *Environ. Sci. Pollut. Res. Int.* 1–11.
- Díaz, J., Linares, C., Carmona, R., Russo, A., Ortiz, C., Salvador, P., Trigo, R.M., 2017. Saharan dust intrusions in Spain: health impacts and associated synoptic conditions. *Environ. Res.* 156, 455–467.
- Feretti, D., Pedrazzani, R., Ceretti, E., Grande, M.Dal, Zerbini, I., Viola, G.C.V., Gelatti, U., Donato, F., Zani, C., 2019. Risk is in the air": polycyclic aromatic hydrocarbons, metals and mutagenicity of atmospheric particulate matter in a town of Northern Italy (Respira study). *Mutat. Res. Genet. Toxicol. Environ. Mutagen.* 842, 35–49.

- Fernández-Raga, M., Díaz-Marugán, L., García Escolano, M., Bort, C., Fanjul, V., 2021. SARS-CoV-2 viability under different meteorological conditions, surfaces, fluids and transmission between animals. *Environ. Res.* 192, 110293.
- Gangwar, R.S., Bevan, G.H., Palanivel, R., Das, L., Rajagopalan, S., 2020. Oxidative stress pathways of air pollution mediated toxicity: recent insights. *Redox Biol.* 34, 101545.
- Gentner, D.R., Jathar, S.H., Gordon, T.D., Bahreini, R., Day, D.A., El Haddad, I., Hayes, P.L., Pieber, S.M., Platt, S.M., de Gouw, J., Goldstein, A.H., Harley, R.A., Jimenez, J.L., Prévôt, A.S., Robinson, A.L., 2017. Review of urban secondary organic aerosol formation from gasoline and diesel motor vehicle emissions. *Environ. Sci. Technol.* 51, 1074–1093.
- Gerba, C.P., 1984. Applied and theoretical aspects of virus adsorption to surfaces. *Adv. Appl. Microbiol.* 30, 133–168.
- Gómez, A., Armas, O., Lilik, G.K., Boehman, A., 2012. Estimation of volatile organic emission based on diesel particle size distributions. *Meas. Sci. Technol.* 23, 105305.
- Greenhalgh, T., Jimenez, J.L., Prather, K.A., Tufekci, Z., Fisman, D., Schooley, R., 2021. Ten scientific reasons in support of airborne transmission of SARS-CoV-2. *Lancet* 397, 1603–1605.
- Groulx, N., Urch, B., Duchaine, C., Mubareka, S., Scott, J.A., 2018. The Pollution Particulate Concentrator (PopCon): a platform to investigate the effects of particulate air pollutants on viral infectivity. *Sci. Total Environ.* 628–629, 1101–1107.
- Haynes, B.S., Wagner, H.G., 1981. Soot formation. *Prog. Energy Combust. Sci.* 7, 229–273.
- Jaworski, A., Kuszewski, H., Ustrzycki, A., Balawender, K., Lejda, K., Woś, P., 2018. Analysis of the repeatability of the exhaust pollutants emission research results for cold and hot starts under controlled driving cycle conditions. *Environ. Sci. Pollut. Res. Int.* 25, 17862–17877.
- Karjalainen, P., Timonen, H., Saukko, E., Kuuluvainen, H., Saarikoski, S., Aakko-Saksa, P., Murtonen, T., Bloss, M., Dal Maso, M., Simonen, P., Ahlberg, E., Svenningsson, B., Brune, W.H., Hillamo, R., Keskinen, J., Rönkkö, T., 2016. Time-resolved characterization of primary particle emissions and secondary particle formation from a modern gasoline passenger car. *Atmos. Chem. Phys.* 16, 8559–8570.
- Korom, M., Wylie, K.M., Morrison, L.A., 2008. Selective ablation of virion host shutoff protein RNase activity attenuates herpes simplex virus 2 in mice. *J. Virol.* 82, 3642–3653.
- Lara, S., Villanueva, F., Martín, P., Salgado, S., Moreno, A., Sánchez-Verdú, P., 2022. Investigation of PAHs, nitrated PAHs and oxygenated PAHs in PM10 urban aerosols. A comprehensive data analysis. *Chemosphere* 294, 133745.
- Lembo, R., Landoni, G., Cianfanelli, L., Frontera, A., 2021. Air pollutants and SARS-CoV-2 in 33 European countries. *Acta Biomed.* 92, e2021166.
- Lewtas, J., 2007. Air pollution combustion emissions: characterization of causative agents and mechanisms associated with cancer, reproductive, and cardiovascular effects. *Mutat. Res. Rev. Mutat. Res.* 636, 95–133.
- Li, H., Xu, X.L., Dai, D.W., Huang, Z.Y., Ma, Z., Guan, Y.J., 2020. Air pollution and temperature are associated with increased COVID-19 incidence: a time series study. *Int. J. Infect. Dis.* 97, 278–282.
- Li, Z., Tao, B., Hu, Z., Yi, Y., Wang, J., 2022. Effects of short-term ambient particulate matter exposure on the risk of severe COVID-19. *J. Infect.* 84 (5), 684–691.
- Liu, H., Zhang, X., Zhang, H., Yao, X., Zhou, M., Wang, J., He, Z., Zhang, H., Lou, L., Mao, W., Zheng, P., Hu, B., 2018. Effect of air pollution on the total bacteria and pathogenic bacteria in different sizes of particulate matter. *Environ. Pollut.* 233, 483–493.
- Lv, Q., Liu, M., Qi, F., Gong, S., Zhou, S., Zhan, S., Bao, L., 2020. Sensitivity of SARS-CoV-2 to different temperatures. *Anim. Models Exp. Med.* 3, 316–318.
- Maleki, M., Anvari, E., Hopke, P.K., Noorimotlagh, Z., Mirzaee, S.A., 2021. An updated systematic review on the association between atmospheric particulate matter pollution and prevalence of SARS-CoV-2. *Environ. Res.* 195, 110898.
- Manisalidis, I., Stavropoulou, E., Stavropoulos, A., Bezirtzoglou, E., 2020. Environmental and health impacts of air pollution: a review. *Front. Public Health* 8, 14.
- Mescoli, A., Maffei, G., Pillo, G., Bortone, G., Marchesi, S., Morandi, E., Ranzi, A., Rotondo, F., Serra, S., Vaccari, M., Sajani, S., Zauli, M., Mascolo, M.G., Jacobs, M.N., Colacci, A.A., 2020. The secretive liaison of particulate matter and SARS-CoV-2. A hypothesis and theory investigation. *Front. Genet.* 11, 579964.
- Mizutani, T., Fukushi, S., Iizuka, D., Inanami, O., Kuwabara, M., Takashima, H., Yanagawa, H., Saijo, M., Kurane, I., Morikawa, S., 2006. Inhibition of cell proliferation by SARS-CoV infection in Vero E6 cells. *FEMS Immunol. Med. Microbiol.* 46, 236–243.
- Momenimovahed, A., Olfert, J.S., 2015. Effective density and volatility of particles emitted from gasoline direct injection vehicles and implications for particle mass measurement. *Aerosol Sci. Technol.* 49, 1051–1062.
- Momenimovahed, A., Liu, F., Thomson, K.A., Smallwood, G.J., Guo, H., 2021. Effect of fuel composition on properties of particles emitted from a diesel–natural gas dual fuel engine. *Int. J. Engine Res.* 22, 77–87.
- Oanh, N.T.K., Reutergerardh, L.B., Dung, N.T., 1999. Emission of polycyclic aromatic hydrocarbons and particulate matter from domestic combustion of selected fuels. *Environ. Sci. Technol.* 33, 2703–2709.
- Omidvarborna, H., Kumar, A., Kim, D.S., 2015. Recent studies on soot modeling for diesel combustion. *Renew. Sustain. Energy Rev.* 48, 635–647.
- Pansini, R., Fornacca, D., 2021. Early spread of COVID-19 in the air-polluted regions of eight severely affected countries. *Atmosphere* 12, 795.
- Prasad, R., Rao Bella, V., 2010. A review on diesel soot emission, its effect and control. *Bull. Chem. React. Eng. Catal.* 5, 69–86.
- Samanthi, U., 2021. What is the difference between NFkB1 and NFkB2. <https://www.differencebetween.com/what-is-the-difference-between-nfkb1-and-nfkb2/>. (Accessed April 2022).
- Santurtún, A., Colom, M.L., Fdez-Arroyabe, P., Real, A.D., Fernández-Olmo, I., Zarrabeitia, M.T., 2022. Exposure to particulate matter: direct and indirect role in the COVID-19 pandemic. *Environ. Res.* 206, 112261.
- Setti, L., Passarini, F., Gennaro, G.De, Barbieri, P., Perrone, M.G., Borelli, M., Palmisani, J., Gilio, A.Di, Torboli, V., Fontana, F., Clemente, L., Pallavicini, A., Ruscio, M., Piscitelli, P., Miani, A., 2020. SARS-Cov-2RNA found on particulate matter of Bergamo in Northern Italy: first evidence. *Environ. Res.* 188, 109754.
- Soriano, J.A., Agudelo, J.R., López, A.F., Armas, O., 2017. Oxidation reactivity and nanostructural characterization of the soot coming from farnesane - a novel diesel fuel derived from sugar cane. *Carbon* 125, 516–529.
- Soriano, J.A., García-Contreras, R., Leiva-Candia, D., Soto, F., 2018. Influence on performance and emissions of an automotive diesel engine fueled with biodiesel and paraffinic fuels: GTL and biojet fuel farnesane. *Energy Fuels* 32, 5125–5133.
- Soriano, J.A., García-Contreras, R., de la Fuente, J., Armas, O., Orozco-Jimenez, L.Y., Agudelo, J.R., 2020. Genotoxicity and mutagenicity of particulate matter emitted from diesel, gas to liquid, biodiesel, and farnesane fuels: a toxicological risk assessment. *Fuel* 282, 118763.
- Stapleton, E.M., Welch, J.L., Ubeda, E.A., Xiang, J., Zabner, J., Thornell, I.M., Nonnenmann, M.W., Stapleton, J.T., Comellas, A.P., 2022. Urban particulate matter impairment of airway surface liquid-mediated coronavirus inactivation. *J. Infect. Dis.* 225, 214–218.
- Traboulsi, H., Guerrina, N., Iu, M., Maysinger, D., Ariya, P., Baglole, C.J., 2017. Inhaled pollutants: the molecular scene behind respiratory and systemic diseases associated with ultrafine particulate matter. *Int. J. Mol. Sci.* 18, 243.
- Tree, D.R., Svenson, K.I., 2007. Soot processes in compression ignition engines. *Prog. Energy Combust. Sci.* 33, 272–309.
- Usemann, J., Roth, M., Bisig, C., Comte, P., Czerwinski, J., Mayer, A.C.R., Latzin, P., Müller, L., 2018. Gasoline particle filter reduces oxidative DNA damage in bronchial epithelial cells after whole gasoline exhaust exposure in vitro. *Sci. Rep.* 8, 2297.
- Villanueva, F., Tapia, A., Cabañas, B., Martínez, E., Albaladejo, J., 2015. Characterization of particulate polycyclic aromatic hydrocarbons in an urban atmosphere of central-southern Spain. *Environ. Sci. Pollut. Res. Int.* 22, 18814–18823.
- Villanueva, F., Lara, S., Amo-Salas, M., Cabañas, B., Martín, P., Salgado, S., 2021. Investigation of formaldehyde and other carbonyls in a small urban atmosphere using passive samplers. A comprehensive data analysis. *Microchem. J.* 167, 106270.
- Villeneuve, P.J., Goldberg, M.S., 2022. Ecological studies of COVID-19 and air pollution: how useful are they? *Environ. Epidemiol.* 6, e195.
- von Schneidmeyer, E., Steinmar, K., Weatherhead, E.C., Bonn, B., Gerwig, H., Quedenau, J., 2019. Air pollution at human scales in an urban environment: impact of local environment and vehicles on particle number concentrations. *Sci. Total Environ.* 688, 691–700.
- Woodby, B., Arnold, M.M., Valacchi, G., 2021. SARS-CoV-2 infection, COVID-19 pathogenesis, and exposure to air pollution: what is the connection? *Ann. N. Y. Acad. Sci.* 1486, 15–38.
- Xin, Y., Grundmeier, G., Keller, A., 2021. Adsorption of SARS-CoV-2 spike protein S1 at oxide surfaces studied by high-speed atomic force microscopy. *Adv. Nanobiomed. Res.* 1, 2170023.
- Zielinska, B., Sagebiel, J., Arnott, W.P., Rogers, C.F., Kelly, K.E., Wagner, D.A., Lighty, J.S., Sarofim, A.F., Palmer, G., 2004. Phase and size distribution of polycyclic aromatic hydrocarbons in diesel and gasoline vehicle emissions. *Environ. Sci. Technol.* 38, 2557–2567.